



Research and Development Technical Report

ECOM- 4395

ADAO21976

AN ANTENNA FOR COMBINED SURVEILLANCE AND FOLIAGE
PENETRATION RADAR - COMSFOR

John J. Borowick

Combat Surveillance & Target Acquisition Laboratory

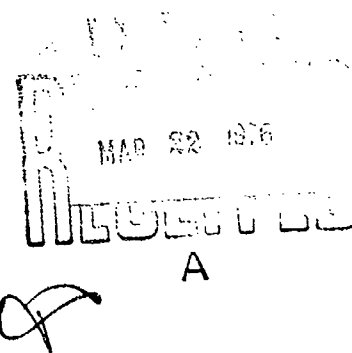
March 1976

DISTRIBUTION STATEMENT

Approved for public release;
distribution unlimited.

ECOM

US ARMY ELECTRONICS COMMAND FORT MONMOUTH, NEW JERSEY 07703



NOTICES

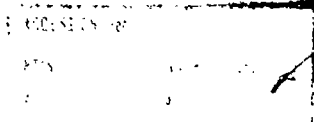
Disclaimers

The findings in this report are not to be construed as an official Department of the Army position, unless so designated by other authorized documents.

The citation of trade names and names of manufacturers in this report is not to be construed as official Government indorsement or approval of commercial products or services referenced herein.

Disposition

Destroy this report when it is no longer needed. Do not return it to the originator.



A

UNCLASSIFIED

SECURITY CLASSIFICATION OF THIS PAGE (When Data Entered)

REPORT DOCUMENTATION PAGE		READ INSTRUCTIONS BEFORE COMPLETING FORM
1. REPORT NUMBER DTIC-1046	2. GOVT ACCESSION NO.	3. RECIPIENT'S CATALOG NUMBER
4. TITLE (and Subtitle) AN ANTENNA FOR COMBINED SURVEILLANCE AND FOLIAGE PENETRATION RADAR - COMSFOR.	5. TYPE OF REPORT & PERIOD COVERED Technical Report.	6. PERFORMING ORG. REPORT NUMBER
7. AUTHOR John/Borowick	8. CONTRACT OR GRANT NUMBER(s) 1-S-762703-DH-93-P-1	9. PROGRAM ELEMENT, PROJECT, TASK AREA & WORK UNIT NUMBERS DAJST-62703-DH93-P-07
10. PERFORMING ORGANIZATION NAME AND ADDRESS US Army Electronics Command ATTN: DESSEL-CT-1 Fort Monmouth, NJ 07703	11. REPORT DATE March 1976	12. NUMBER OF PAGES 21
13. CONTROLLING OFFICE NAME AND ADDRESS US Army Electronics Command CS&TA Laboratory (DESSL-CT-R) Fort Monmouth, NJ 07703	14. MONITORING AGENCY NAME & ADDRESS (if different from Controlling Office) 12 26 p.	15. SECURITY CLASS. (of this report) Unclassified
16. DISTRIBUTION STATEMENT (of this Report) Approved for public release; distribution unlimited.		15a. DECLASSIFICATION/DOWNGRADING SCHEDULE N/A
17. DISTRIBUTION STATEMENT (of the abstract entered in Block 20, if different from Report)		
18. SUPPLEMENTARY NOTES		
19. KEY WORDS (Continue on reverse side if necessary and identify by block number) Antennas Foliage Penetration Radar		
20. ABSTRACT (Continue on reverse side if necessary and identify by block number) An antenna has been designed for the Combined Surveillance and Foliage Penetration Radar (COMSFOR) project. The antenna provides an existing X-band surveillance radar with a moderate foliage penetration capability. The foliage penetration antenna is an array of L-band, stripline dipole/director elements placed in front of an X-band aperture. A description of the dual-frequency antenna is given along with the measured RF performance at both		

DD FORM 1473


EDITION OF 1 NOV 65 IS OBSOLETE

UNCLASSIFIED
SECURITY CLASSIFICATION OF THIS PAGE (When Data Entered)

037620

Cont'd
UNCLASSIFIED

SECURITY CLASSIFICATION OF THIS PAGE(When Data Entered)

frequency bands. A separate L-band corner reflector antenna design which can be mounted on a lightweight telescoping mast is also described. The antenna has demonstrated excellent gain and pattern characteristics for its size. 

UNCLASSIFIED

SECURITY CLASSIFICATION OF THIS PAGE(When Data Entered)

TABLE OF CONTENTS

INTRODUCTION	1
DUAL FREQUENCY ANTENNA	1
L-BAND CORNER REFLECTOR ANTENNA	3
CONCLUSIONS	4
ACKNOWLEDGEMENTS	4

LIST OF ILLUSTRATIONS

Figure

1. COMSPOR Dual Frequency Antenna	5
2. Measured radiation pattern, L-band Array, sum and difference feed, 1250 MHz, E-plane	6
3. Measured radiation pattern, L-band array, 1250 MHz, H plane	7
4. Measured radiation pattern, single dipole/director element symmetrically placed over X-band aperture, 1250 MHz, E, H plane	8
5. Measured impedance, single dipole/director element over X-band aperture	9
6. Measured impedance, complete L-band antenna over X-band aperture	10
7. Measured impedance, stripline hybrid ring with 50-ohm coaxial loads on antenna ports	11
8. Measured radiation pattern, X-band antenna without L-band antenna in place 9.3 GHz, E plane	12
9. Measured radiation pattern, X-band antenna without L-band antenna in place, 9.3 GHz, H plane	13
10. Measured radiation pattern, X-band antenna with L-band antenna in place, 9.3 GHz, E plane	14
11. Measured radiation pattern, X-band antenna with L-band antenna in place, 9.3 GHz, H plane	15
12. Measured impedance, X-band antenna, with and without L-band array in place	16
13. L-band Corner Reflector Antenna	17
14. Measured radiation pattern, L-band corner reflector antenna, sum and difference feed, 1250 MHz, E plane	18
15. Measured radiation pattern, L-band corner reflector antenna, 1250 MHz, H plane	19
16. Measured impedance, L-band corner reflector antenna 1200 - 1300 MHz	20
17. L-band corner reflector antenna gain	21

TABLE OF CONTENTS

Page

INTRODUCTION	1
DUAL FREQUENCY ANTENNA	1
L-BAND CORNER REFLECTOR ANTENNA	3
CONCLUSIONS	4
ACKNOWLEDGEMENT	4

LIST OF ILLUSTRATIONS

Figure

1. COMPFOR Dual Frequency Antenna	5
2. Measured radiation pattern, L-band Array, sum and difference feed, 1250 MHz, E-plane	6
3. Measured radiation pattern, L-band array, 1250 MHz, H plane	7
4. Measured radiation pattern, single dipole/director element symmetrically placed over X-band aperture, 1250 MHz, E, H plane	8
5. Measured impedance, single dipole/director element over X-band aperture	9
6. Measured impedance, complete L-band antenna over X-band aperture	10
7. Measured impedance, stripline hybrid ring with 50-ohm coaxial loads on antenna ports	11
8. Measured radiation pattern, X-band antenna without L-band antenna in place, 9.3 GHz, E plane	12
9. Measured radiation pattern, X-band antenna without L-band antenna in place, 9.3 GHz, H plane	13
10. Measured radiation pattern, X-band antenna with L-band antenna in place, 9.3 GHz, E plane	14
11. Measured radiation pattern, X-band antenna with L-band antenna in place, 9.3 GHz, H plane	15
12. Measured impedance, X-band antenna, with and without L-band array in place	16
13. L-band Corner Reflector Antenna	17
14. Measured radiation pattern, L-band corner reflector antenna, sum and difference feed, 1250 MHz, E plane	18
15. Measured radiation pattern, L-band corner reflector antenna, 1250 MHz, H plane	19
16. Measured impedance, L-band corner reflector antenna 1200 - 1300 MHz	20
17. L-band corner reflector antenna gain	21

INTRODUCTION

One of the basic deficiencies of short range, microwave surveillance radars is their inability to penetrate even moderate foliage. A program has been underway in the Radar Technical Area of the Combat Surveillance and Target Acquisition Laboratory, Fort Monmouth, N.J. to investigate the addition of an L-band foliage penetration array to an existing X-band surveillance radar antenna. The objective was to achieve this capability without appreciably adding to the size or weight of the X-band antenna. The acronym COMSFOR was coined to designate this Combined Surveillance and Foliage Penetration Radar which resulted from the experiment.

Another L-band array, designed to provide more gain, was to be used for foliage penetration alone. This antenna was also designed to be lightweight, but capable of being mounted atop a man-portable mast, separate from the X-band antenna.

The design of each antenna and the results obtained are described in this report.

DUAL FREQUENCY ANTENNA

The experimental model developed for the Combined Surveillance and Foliage Penetration Radar dual-frequency antenna is shown in Figure 1. The X-band antenna is a flat plate array of broadwall waveguide slots. The array is mounted on a lightweight tripod and is mechanically scanned in azimuth. The antenna radiates with vertical polarization in the scan plane. There is no electronic or mechanical scan in elevation. The foliage penetration antenna was designed for L-band (1220-1280 MHz) for somewhat lesser attenuation through the foliage and therefore better radiation penetration than that possible with the X-band array.

The L-band array consists of four stripline dipole elements, horizontally polarized, each with a passive director. The feed network includes a hybrid ring to provide for phase monopulse in azimuth. The X-band array serves as a reflector when the radar is in the foliage penetration mode. The dipole/director elements are arranged in two pairs, as shown in Figure 1, and are collapsible over each other and in front of the X-band antenna for protection and for convenience of transport. A mechanical lever arrangement is combined with a stripline-to-coax connector for rigidity of the dielectric material and to permit collapsing of the antenna. The mechanical leverage does not interfere with the performance of the antenna. When folding or unfolding the antenna, no RF connections or disconnections are necessary.

The stripline dipole/director elements are printed on two sheets of 0.062-inch thick copper-plated Duroid dielectric. It was found that additional rigidity could be given the dielectric sheets by placing small rivets alongside the radiators and transmission line. The rivets caused no change in the element's radiation or impedance characteristics.

The coax-stripline connector at either short edge of the dielectric excites a 50-ohm stripline transmission line which runs along and close to the long edge of the sheet, to a 90-degree radius band, then serves as the inner conductor of a two arm balun to excite its dipole. The transmission line is

terminated at the dipole. Each coax-stripline connector has attached to it a flexible coaxial cable for continuation of the transmission line to the inside of the radar console. In the final model there would then be an RF bulkhead connector for each of the four flexible cables. Inside the radar console there is a semi-rigid coax cable which continues the transmission line to a stripline hybrid ring "rat race." Integrated with the hybrid is a matching transformer which mates each of the upper and lower dipole/director elements to one of the hybrid's antenna ports.

• The L-band array was designed to provide horizontally-polarized phase monopulse in azimuth over a 1220-1280 MHz band; Figure 2 shows the sum and difference excitation modes plotted on polar log paper for the center frequency. The patterns at the band edges are essentially the same, maintaining both a deep null on the difference pattern and pattern symmetry. The elevation pattern of the array is given in Figure 3. That the aperture has been efficiently used is seen by comparing the measured gain with the directivity of a uniformly illuminated area the size of the X-band aperture. The X-band aperture measures approximately 8 X 13.5 inches. If this area were uniformly illuminated at L-band, the directivity would be 11.8 dB. The measured gain of the stripline dipole/director array over this area used as a reflector is 11 dB across the band. This measured gain includes RF losses in the hybrid ring, the semi-rigid cable from the bulkhead connector to the edge of the stripline board, and the stripline transmission line to the dipole.

The pattern of a single dipole/director element by itself over the center of the X-band aperture is shown in Figure 4. The measured element gain is 8.4 dB with respect to an isotropic point source. It has been noted that the full array of four elements provides only about 3 dB more in gain over that of a single dipole/director element. This is due to the aperture sharing of the individual elements, that is, doubling the number of these elements does not actually double the effective excitation area, as might be the case for a more directive planar antenna. Figure 5 shows the impedance of the dipole/director element, which is essentially the same with the radiator in the environment of the other L-band elements. Input impedance of the entire L-band array, looking into both the sum and difference arms of the hybrid, is given in Figure 6. Figure 7 shows the input impedance of the same hybrid, but with matched coaxial loads as terminations of the antenna ports.

The X-band aperture, which serves as a reflector when in the L-band mode, has broadwall slots in horizontal waveguide for vertical polarization.

Each of the L-band array pairs is positioned so that the dielectric sheets are centered between the horizontal rows of waveguide line sources of the X-band antenna. That is, there is no physical obstacle directly over any of the slots. Figures 8 and 9 show plotted in relative power (in dB) the unobstructed radiation patterns of the X-band apertures for the elevation and azimuth planes, respectively, at the center frequency at 9.8 GHz. Figures 10 and 11 show the same pattern cuts for the X-band antenna with the L-band antenna in place, also at 9.8 GHz. Observe that the azimuth scan plane is not affected as much as the pattern of the elevation plane. These patterns are representative of those measured at 9.7 and 9.9 GHz for both the obstructed and unobstructed pattern conditions. The measured input impedance of the X-band array for these same two input conditions is shown in Figure 12.

An indication of the optimum placement of the L-band radiators was determined by measuring both impedance and antenna patterns for several E- and H-plane spacings. Gain variations were also noted for the X-band array for the various L-band configurations, for example:

1. Single set of 2 L-band elements placed symmetrically on the elevation centerline of the X-band aperture: gain change -0.5 dB
2. Two sets of 2 L-band elements placed symmetrically above the X-band aperture (3.8" vertical spacing): gain change -1.5 dB
3. Two sets of 2 L-band elements placed symmetrically above the X-band aperture (5.6" vertical spacing): gain change -1.0 dB
4. Three sets of 2 L-band elements placed above the X-band aperture, one set at the elevation center and the other two sets at the upper and lower edges of the aperture: gain change -0.8 dB

Case 1, although it had the least X-band gain degradation, was not chosen because the one set of L-band radiators had a nominal gain of only 9 dB across the band. Cases 3 and 4 were not used because they resulted in higher side and back lobes than tolerable in the L-band elevation plane. Thus, Case 2, while having the greatest X-band gain degradation of the configurations attempted, resulted in the best overall tradeoff when dual frequency characteristics were considered.

L-BAND CORNER REFLECTOR ANTENNA

An L-band antenna for the Combined Surveillance & Foliage Penetration Radar project which could be used separate from the X-band antenna was also designed and built. This antenna would not actually have dual-mode capability, but would be used for the foliage penetration mode alone. The antenna was to have more gain, minimum resistance to wind, and still be light weight so that it could be hoisted atop a lightweight man-portable mast. By raising the antenna, the ground-lobing loss would also be lessened.

The antenna built is a 90-degree corner reflector with four of what are essentially the same dipole/director elements as used in the dual aperture antenna. The reflector is constructed of a grid of cylindrical aluminum rods to satisfy the requirements of light weight and minimum wind resistance. Figure 13 is a photograph of the antenna mounted on a tripod supported mast. The reflector is hinged along its apex, which permits folding of the reflector to protect the elements in transport. The radiators were adjusted in azimuth for optimum gain-pattern-impedance characteristics. Each pair of elements is joined by a 3-dB stripline power splitter which is in turn joined with flexible coaxial cable to a stripline hybrid ring. The reflector projects an area of 30 inches in azimuth by 19 inches in elevation. An azimuth pattern displaying the sum and difference modes at 1250 MHz is given in Figure 14. The patterns at 1220 and 1280 MHz are essentially the same. An elevation pattern is shown in Figure 15. The stripline hybrid ring for this antenna, unlike that of the dual-band antenna, has no additional matching network as part of the same stripline board. This hybrid ring has a maximum VSWR of 1.15 with at least 30 dB isolation across the band. For the complete antenna feed, the

phase is within 5 degrees from hybrid input to each of the antenna connections. Total input impedance is plotted in Figure 16. Gain with respect to isotropic is plotted in Figure 17.

CONCLUSIONS

A lightweight, low cost antenna has been designed for the foliage penetration mode for the COMSFOR project. It has been demonstrated that, through judicious compromise, an existing X-band antenna can be afforded a very desirable dual-band capability, without redesign of the X-band aperture. The dual-band aperture and the separate corner reflector antenna are both undergoing system evaluation.

ACKNOWLEDGEMENTS

The author wishes to express his appreciation to Mr. Charles Schelleng of the R&D Technical Services Activity for the design of the mechanical linkage used with the COMSFOR antenna, and to Mr. Herb Daley of Combat Surveillance and Target Acquisition Laboratories Radar Technical Area, Antenna Techniques Team, for help in the RF measurements.

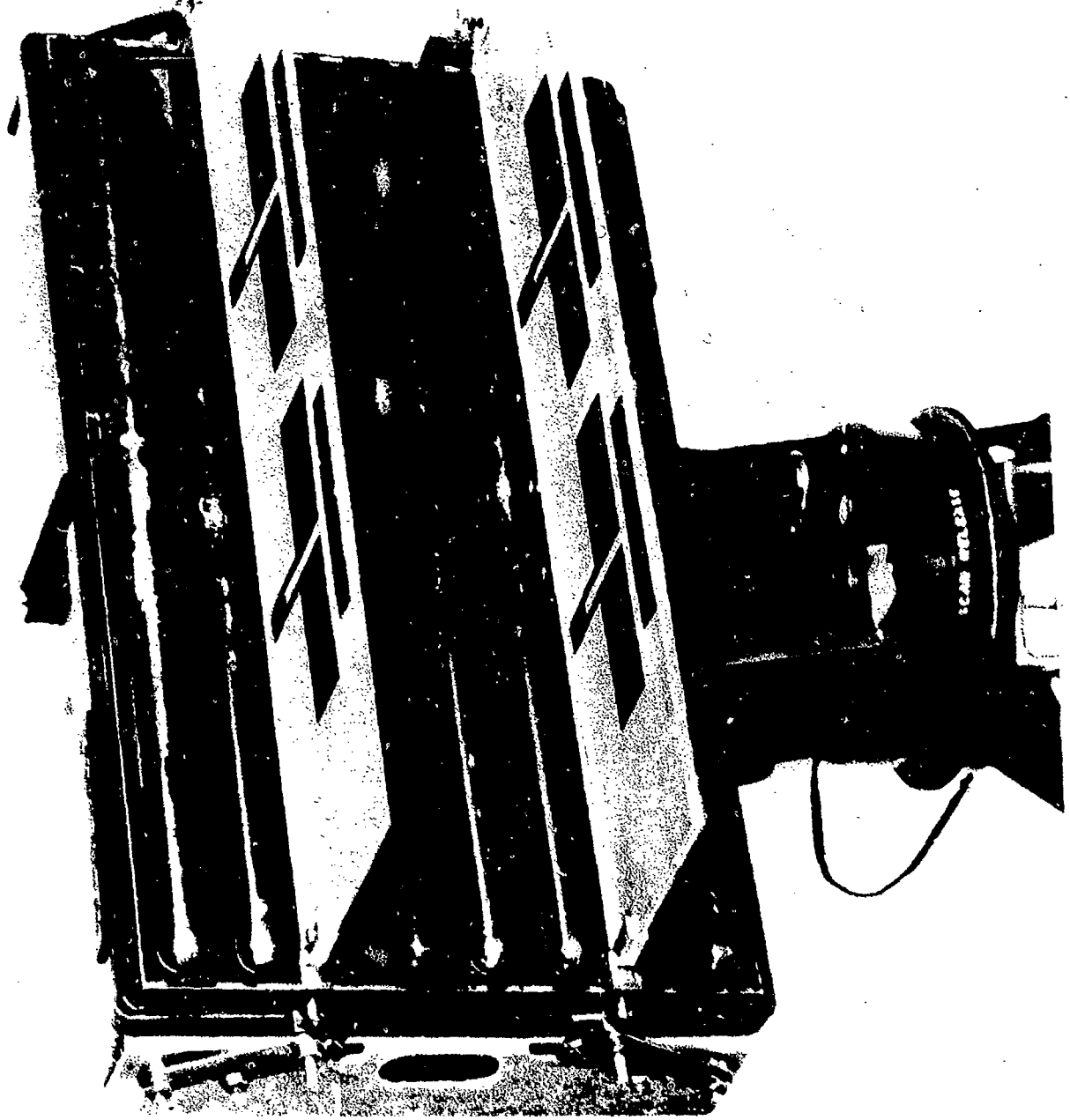


Figure 1. CONSFOR Dual Frequency Antenna

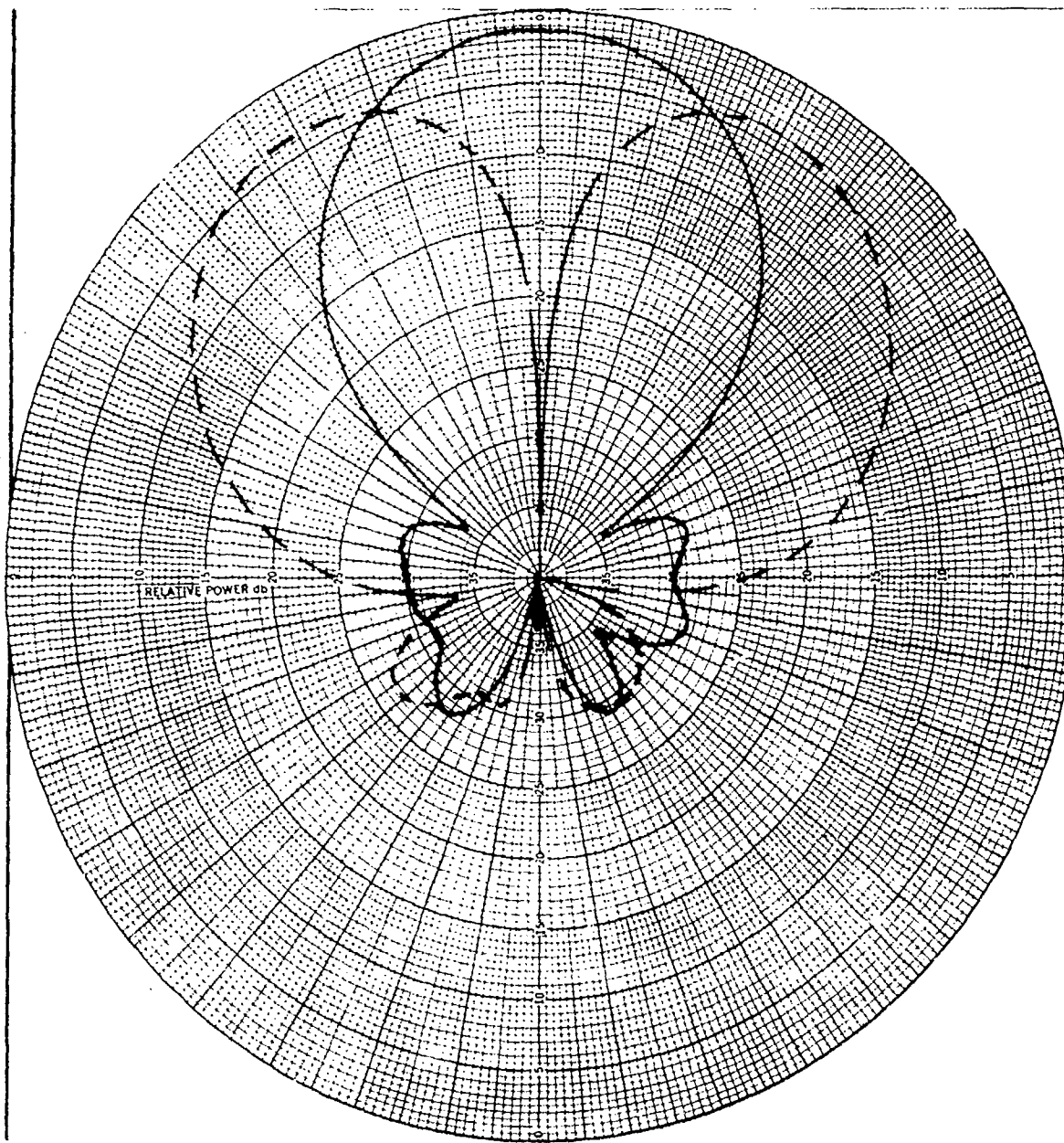


Fig. 2 Measured radiation pattern, L-band Array

————— Sum feed
 - - - - - Difference feed
 1250 MHz, Azimuth (E) plane

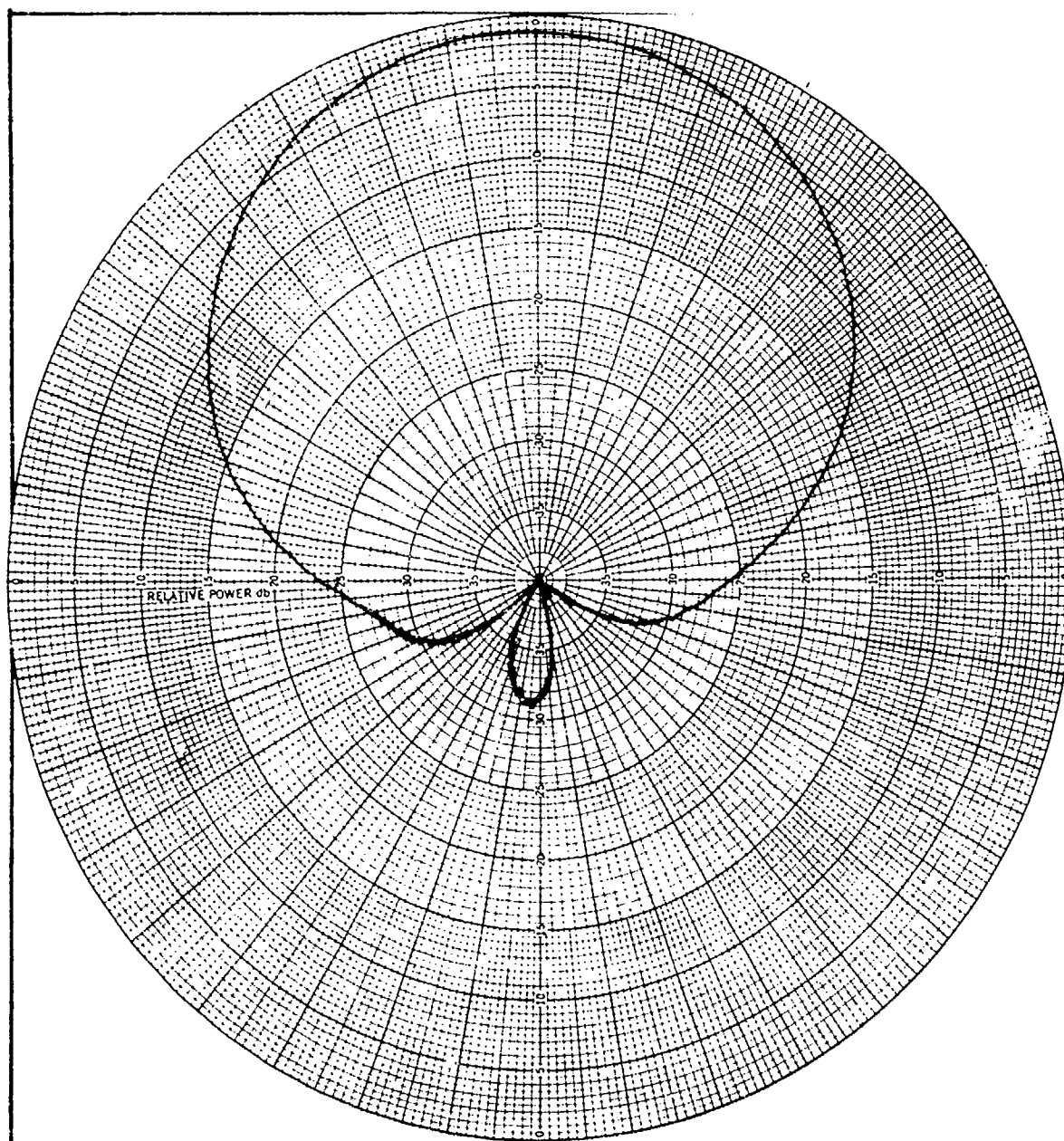


Fig. 3 Measured radiation pattern, L-band Array
1250 MHz, Elevation (H) plane

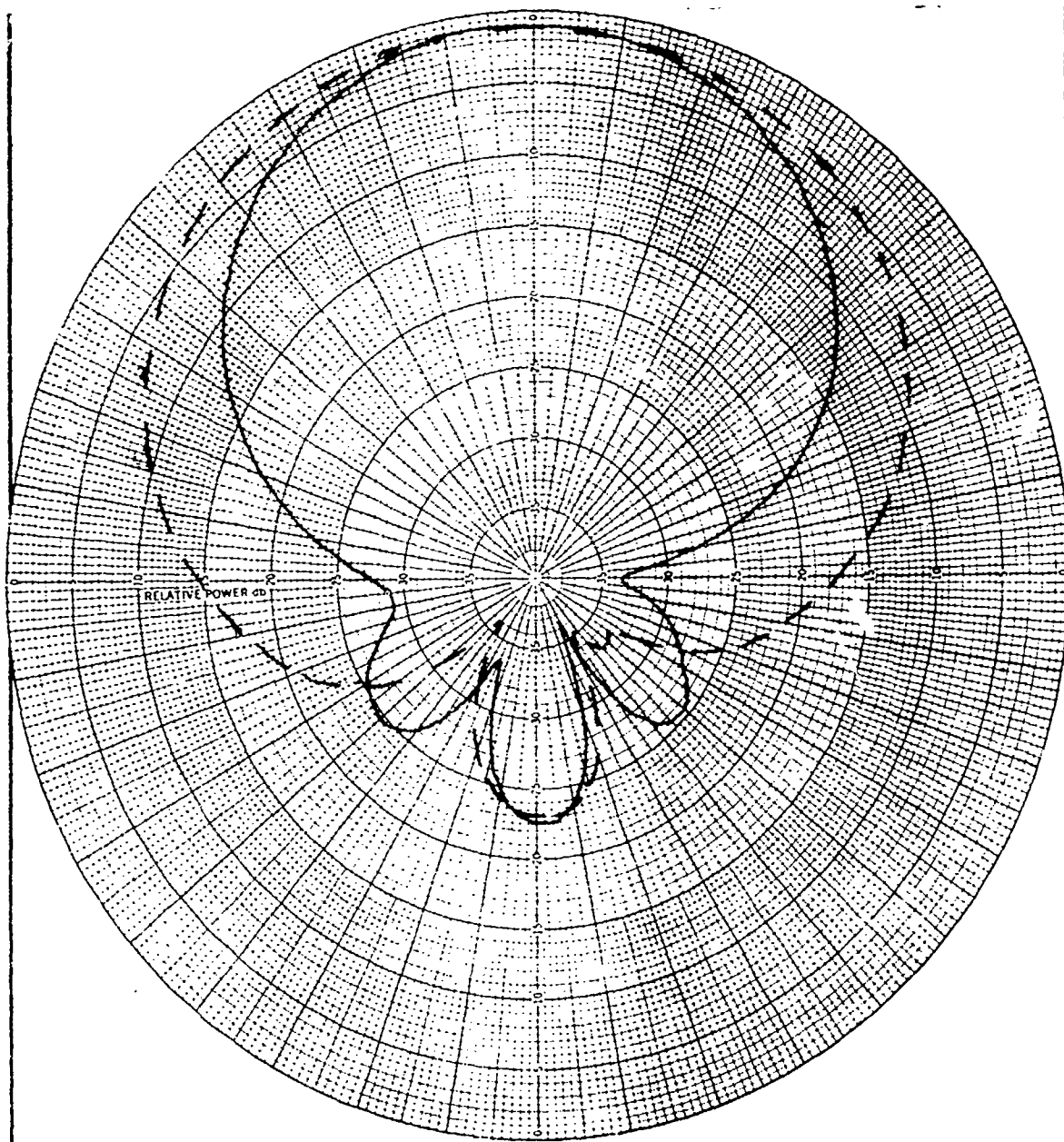


Fig. 4. Measured radiation pattern, single dipole/director element
symmetrically placed over X-band aperture, 1250 MHz

—— Azimuth (E) plane
----- Elevation (H) plane

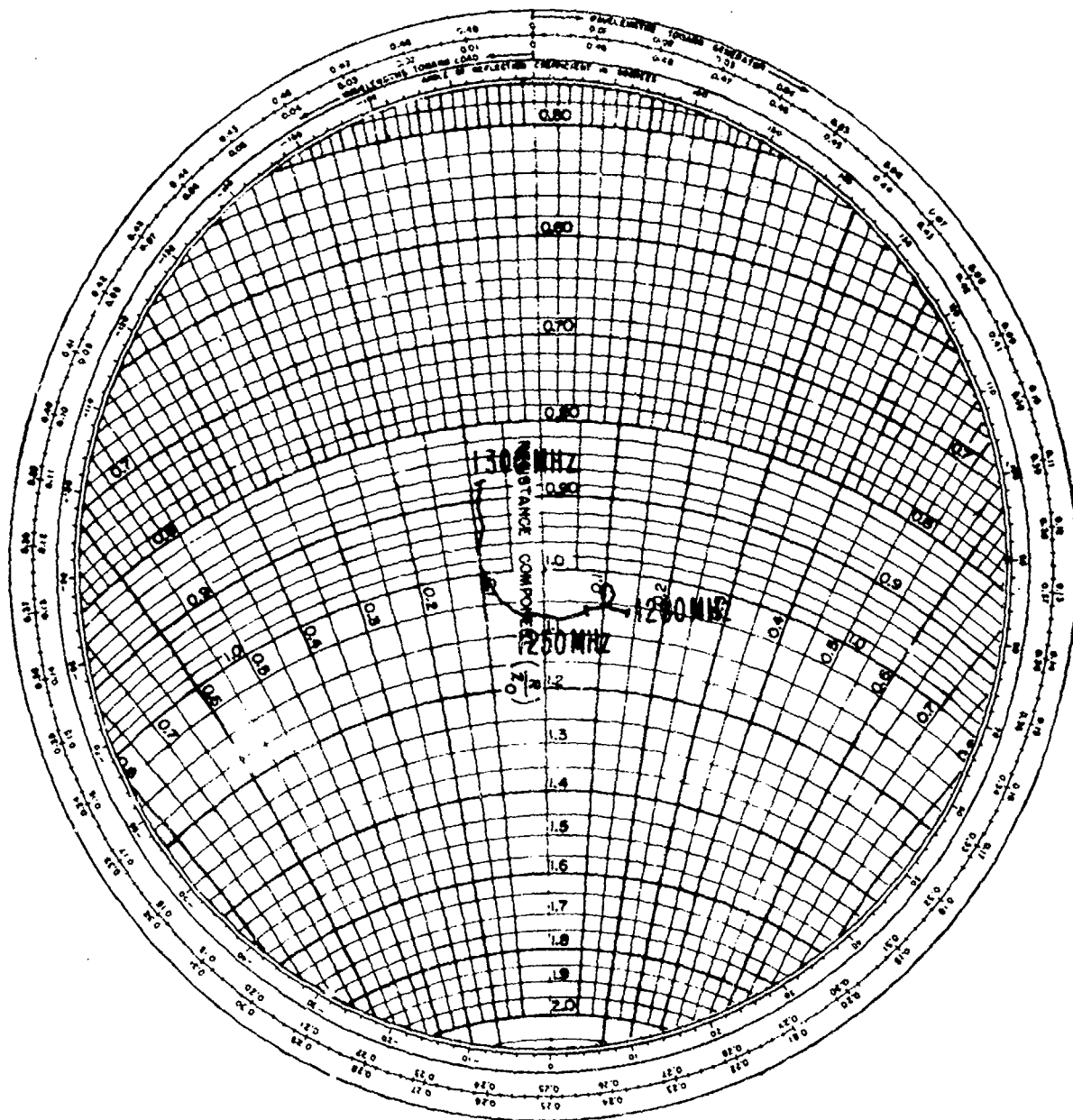


Fig. 5. Measured impedance, single dipole/director element over X-band aperture

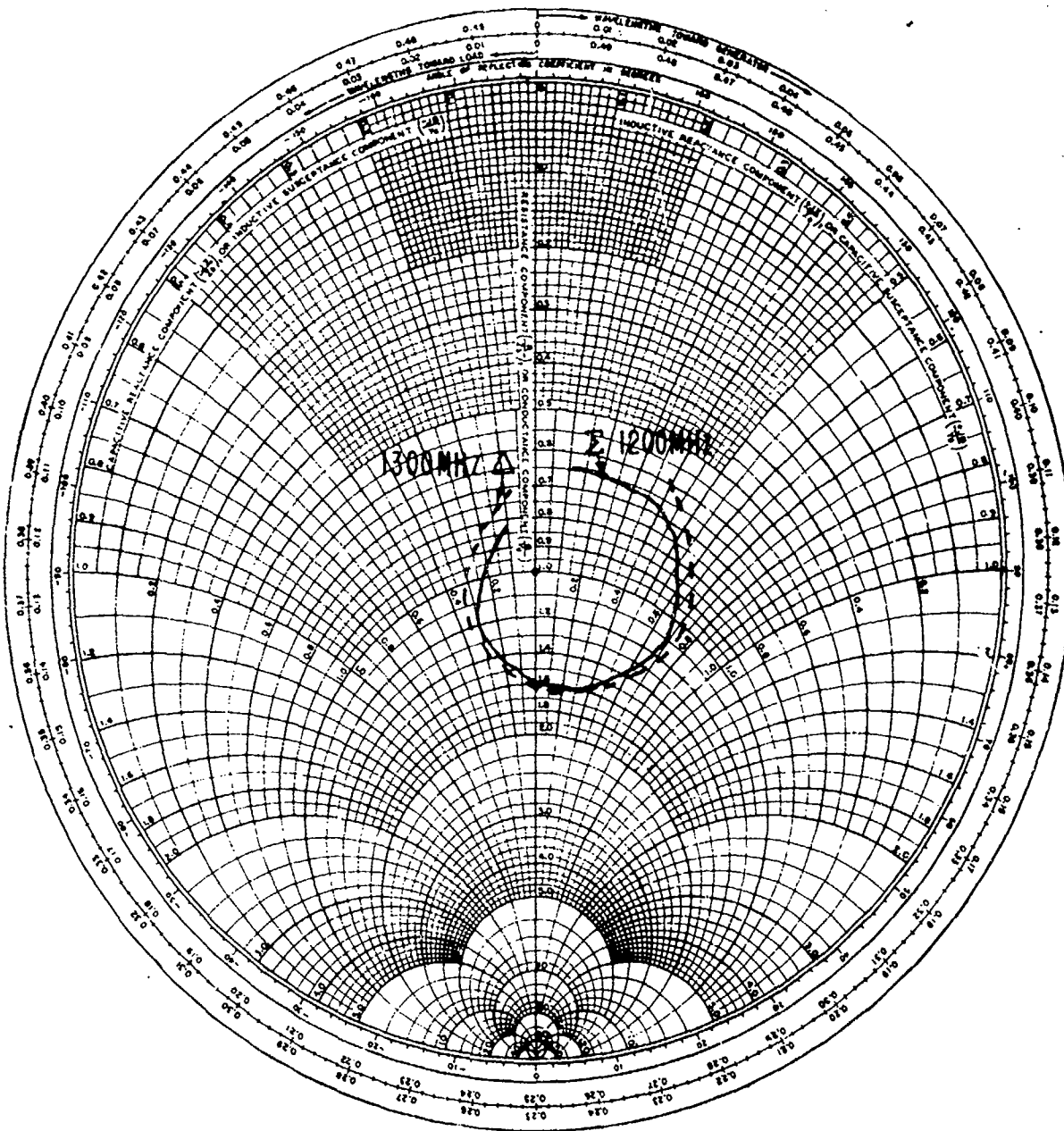


Fig. 6. Measured impedance, complete L-band antenna
over X-band aperture

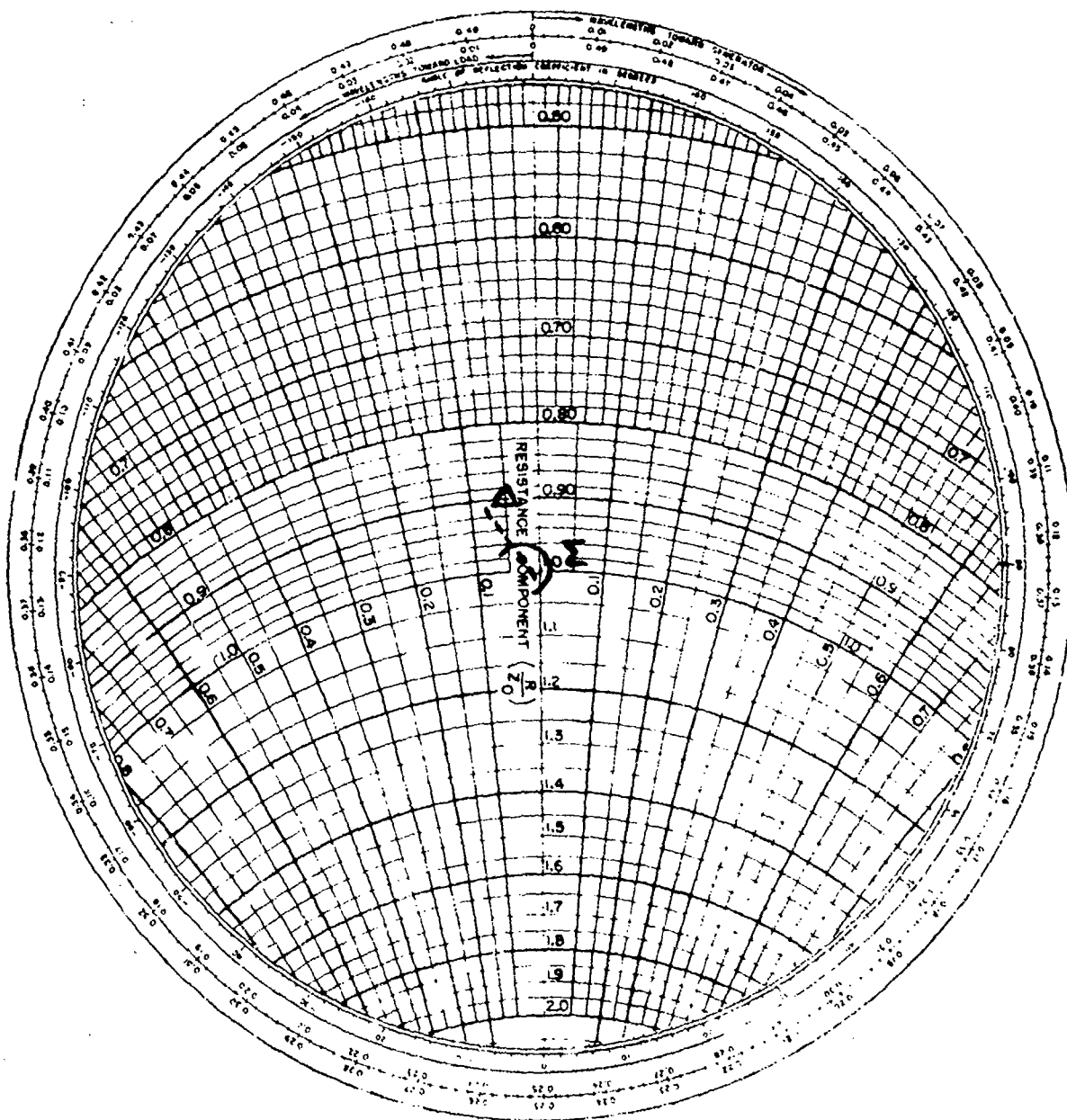


Fig. 7. Measured impedance, stripline hybrid ring
with 50-ohm coaxial loads on antenna ports

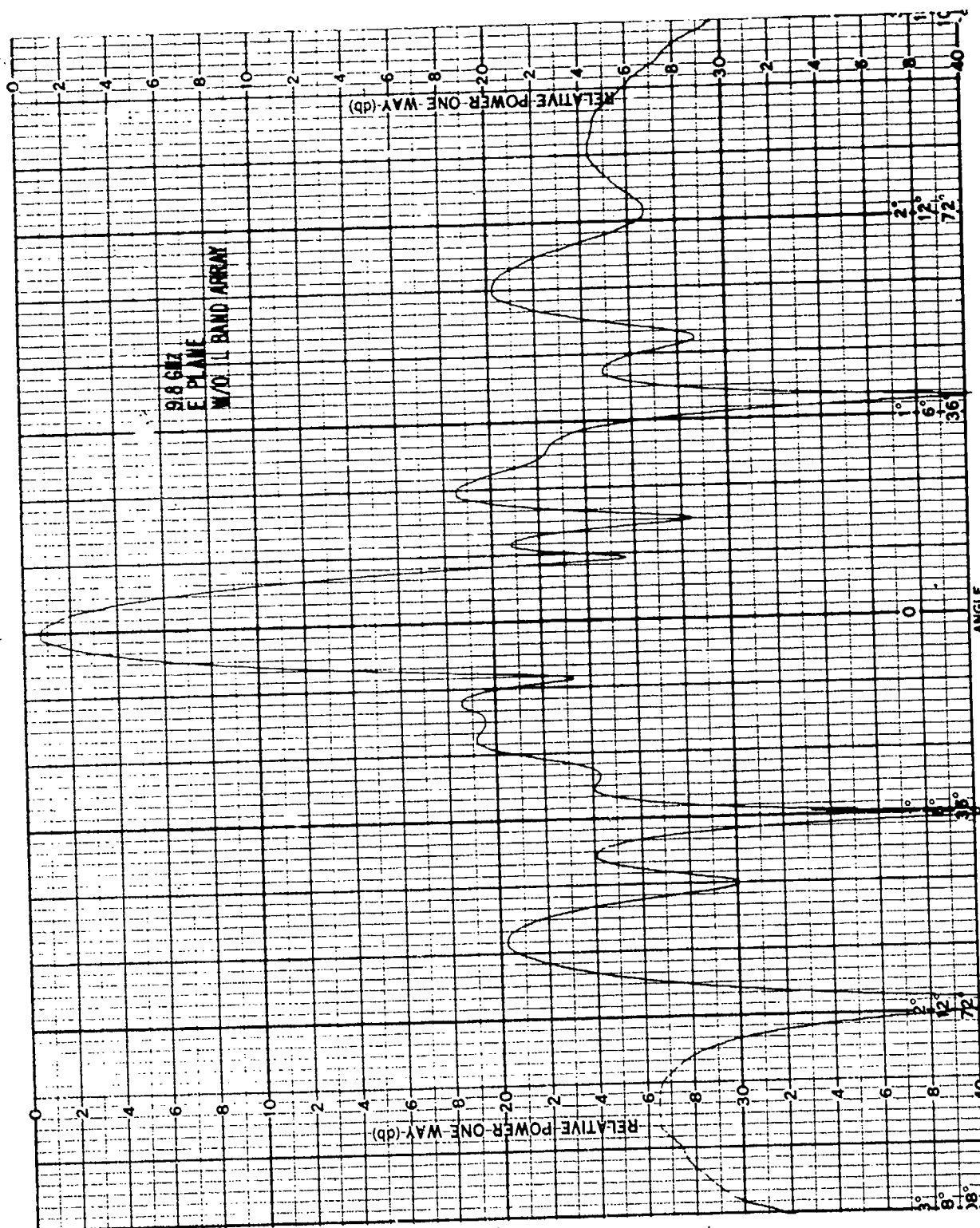


Figure 8. Measured radiation pattern, X-band antenna without L-band antenna in place

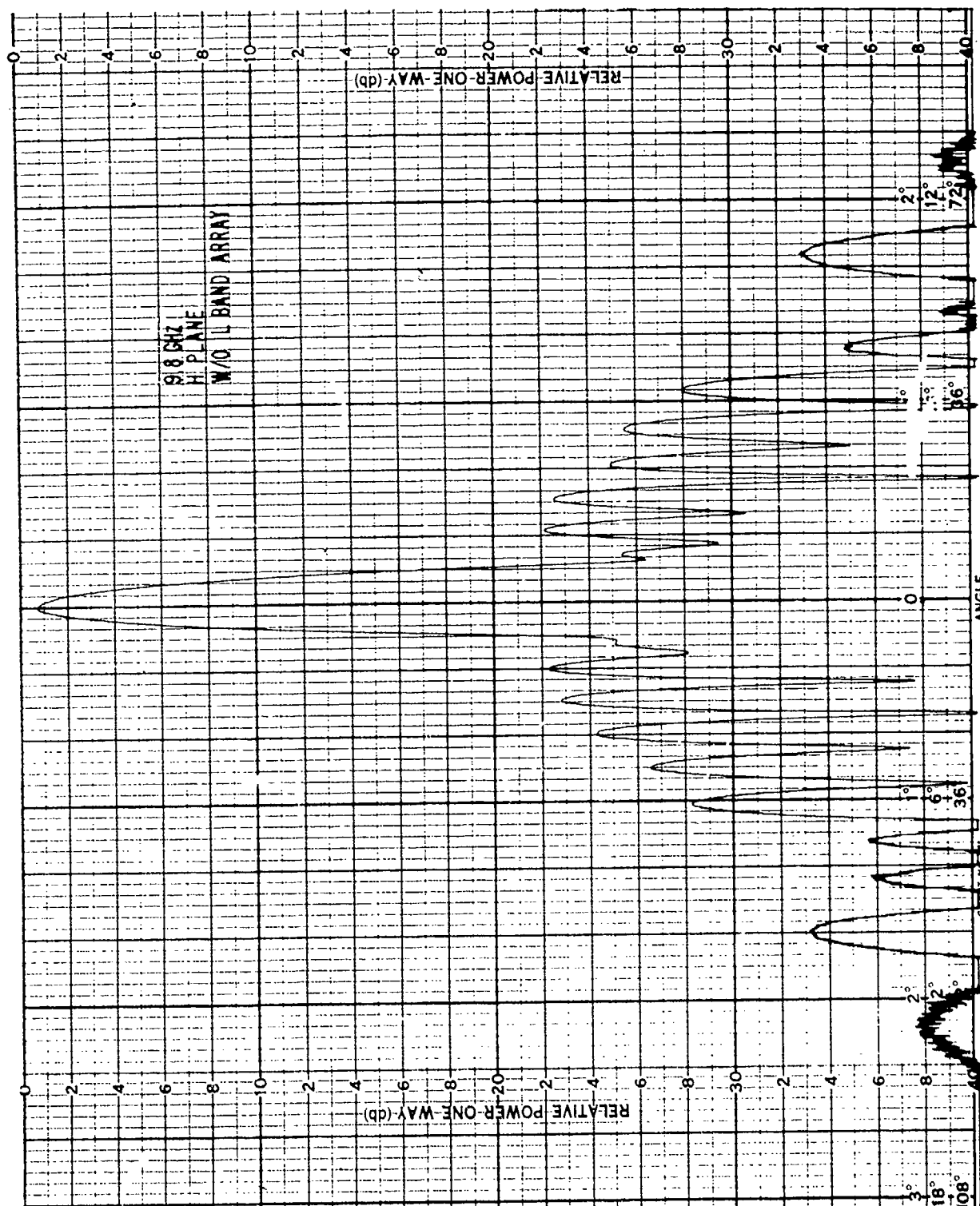


Figure 9. Measured radiation pattern, X-band aperture without L-band antenna in place

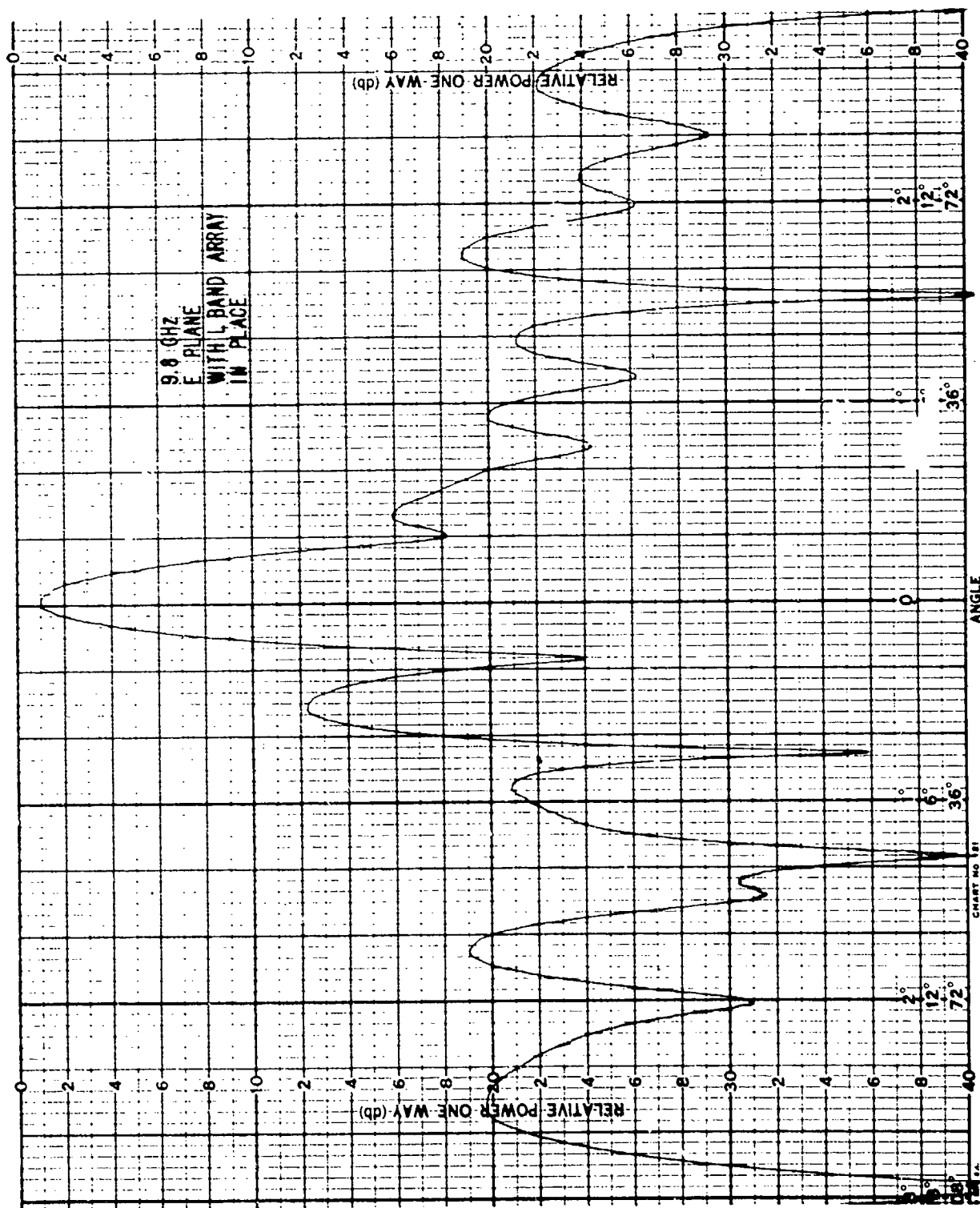


Figure 10. Measured radiation pattern, X-band antenna with L-band antenna in place

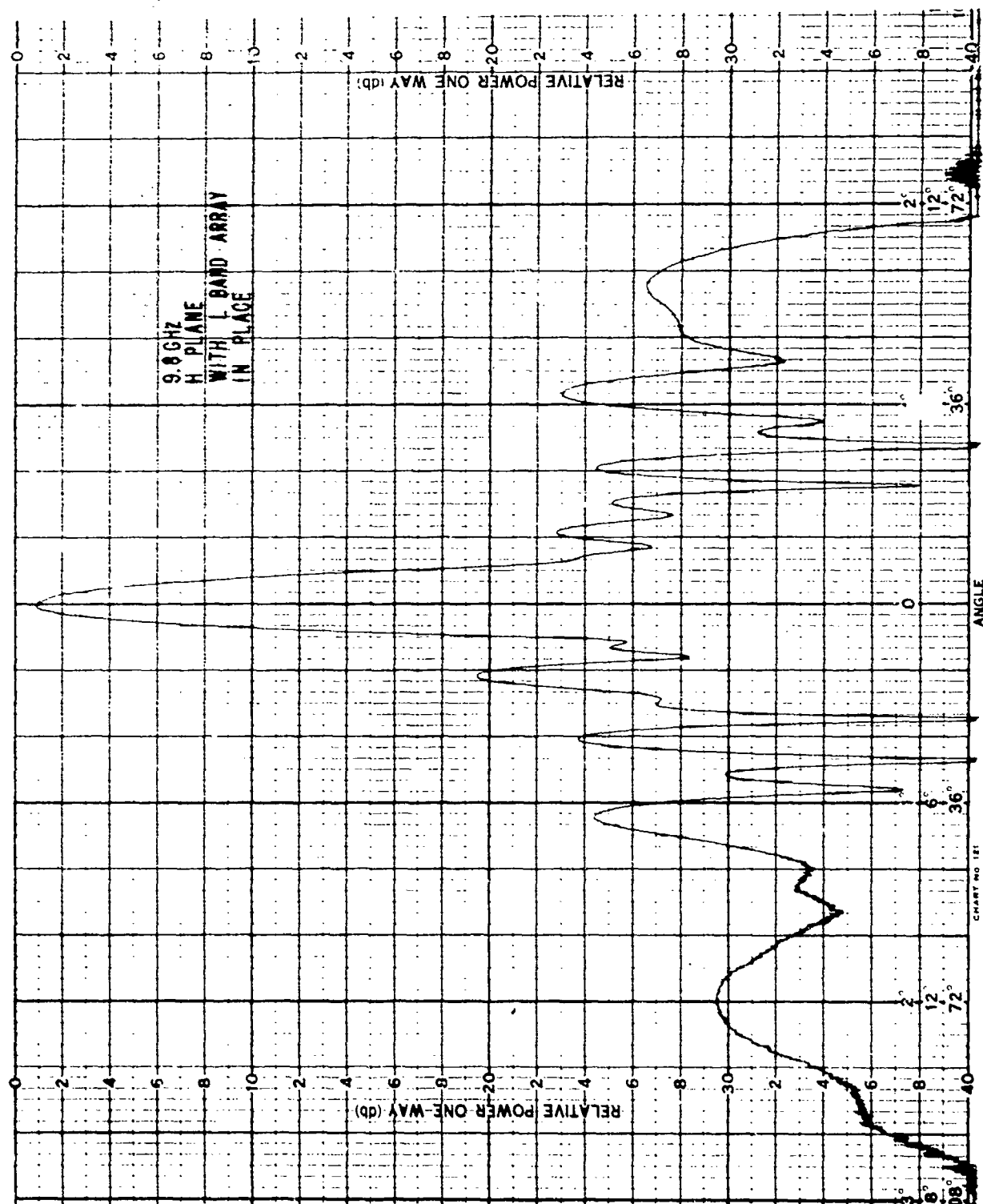


Figure 11. Measured radiation pattern, X-band antenna with L-band antenna in place

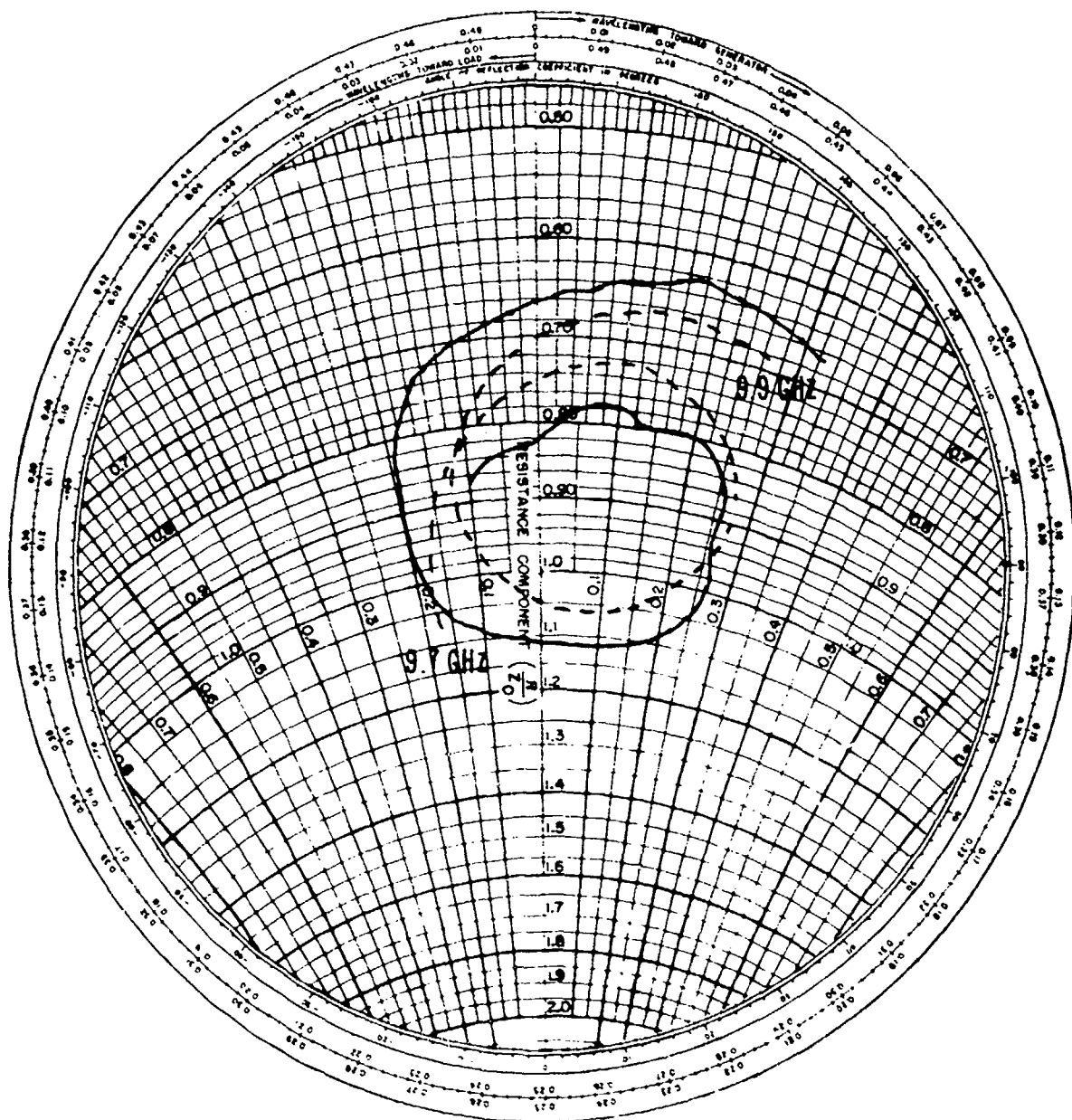


Fig. 12. Measured impedance, X-band antenna
 ——— with L-band array in place
 - - - - - without L-band array in place

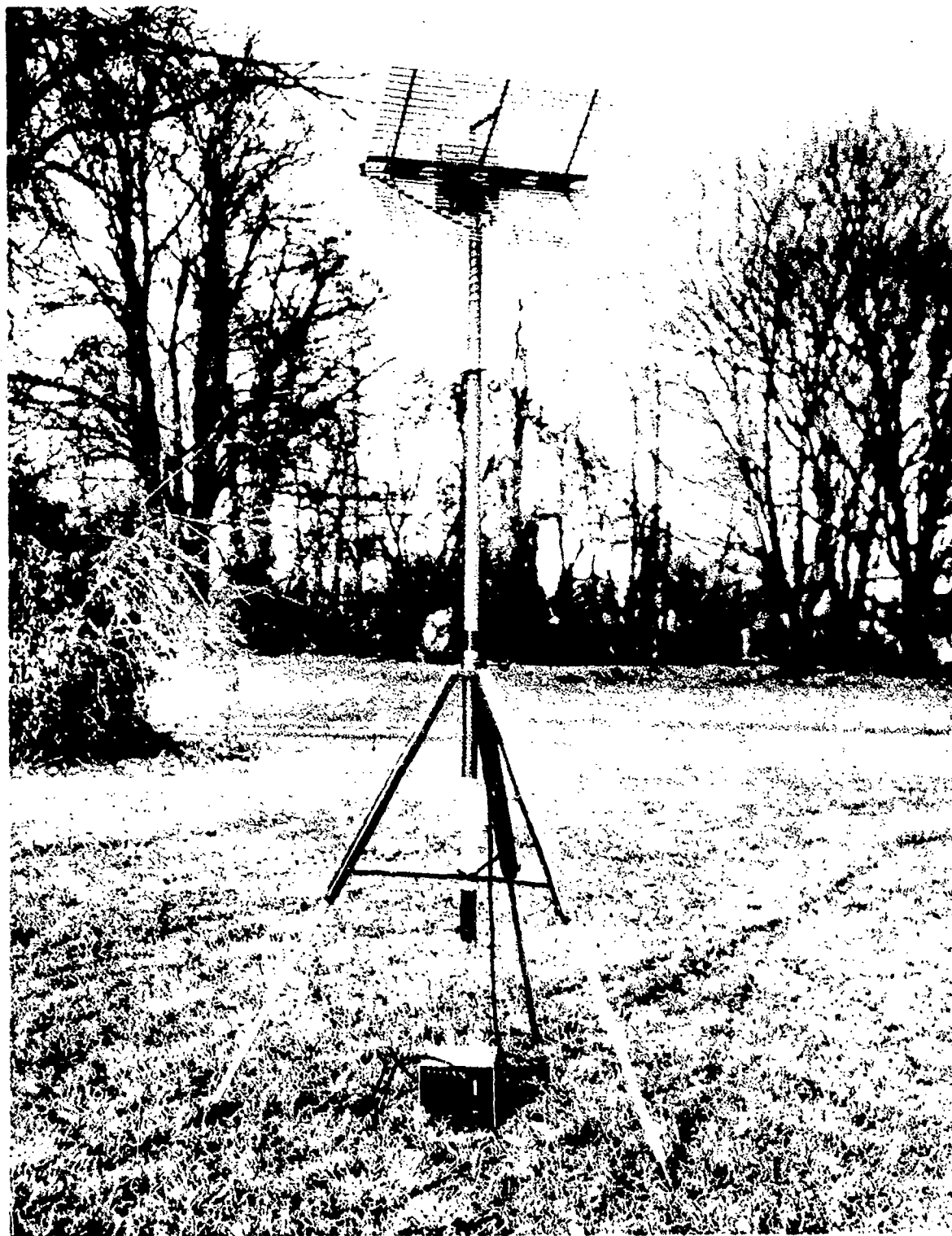


Fig. 13 L-band Corner Reflector Antenna

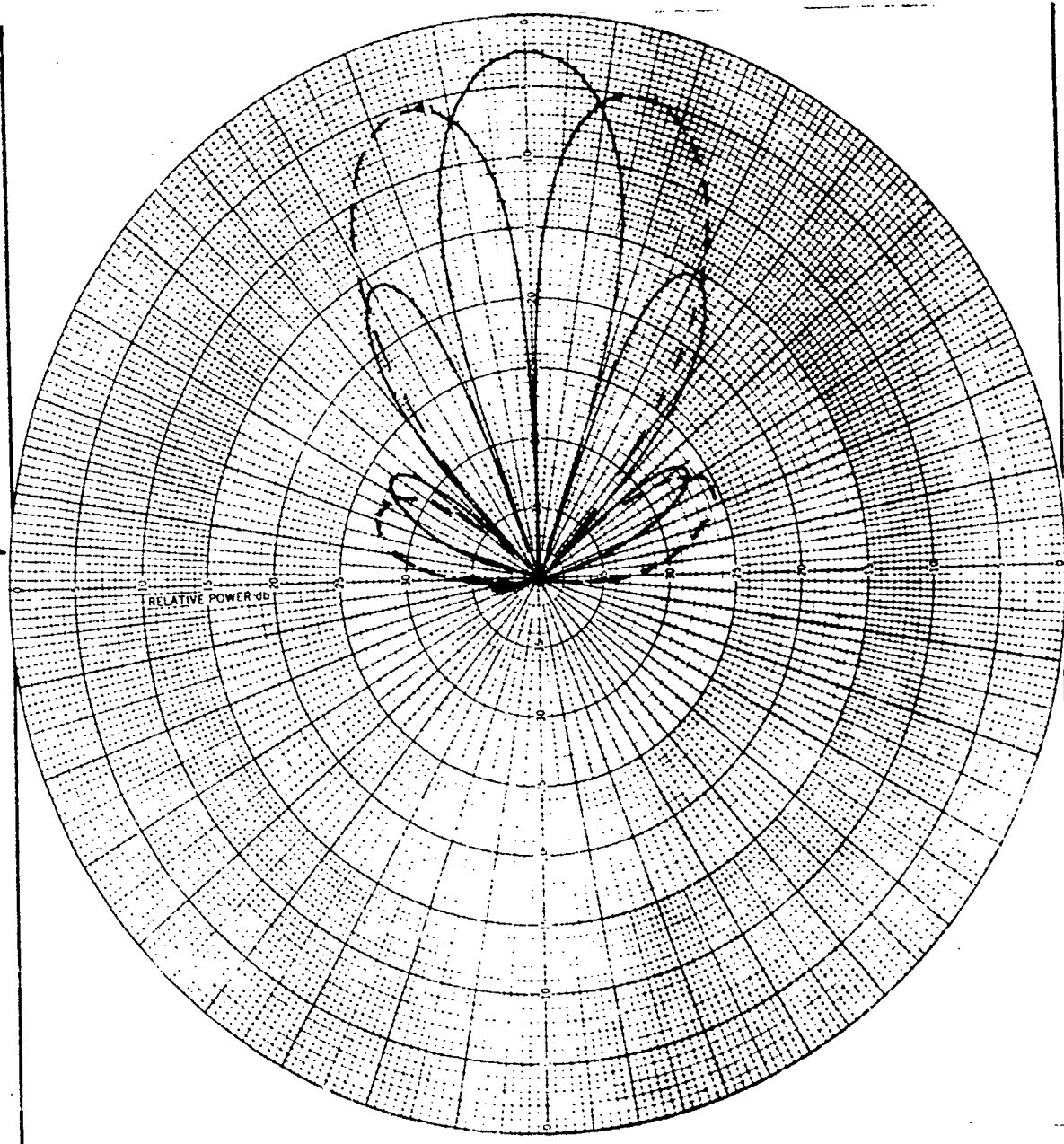


Fig. 14 Measured radiation pattern, L-band corner reflector antenna

—— sum feed
 ----- difference feed
 1250 MHz, Azimuth (E) plane

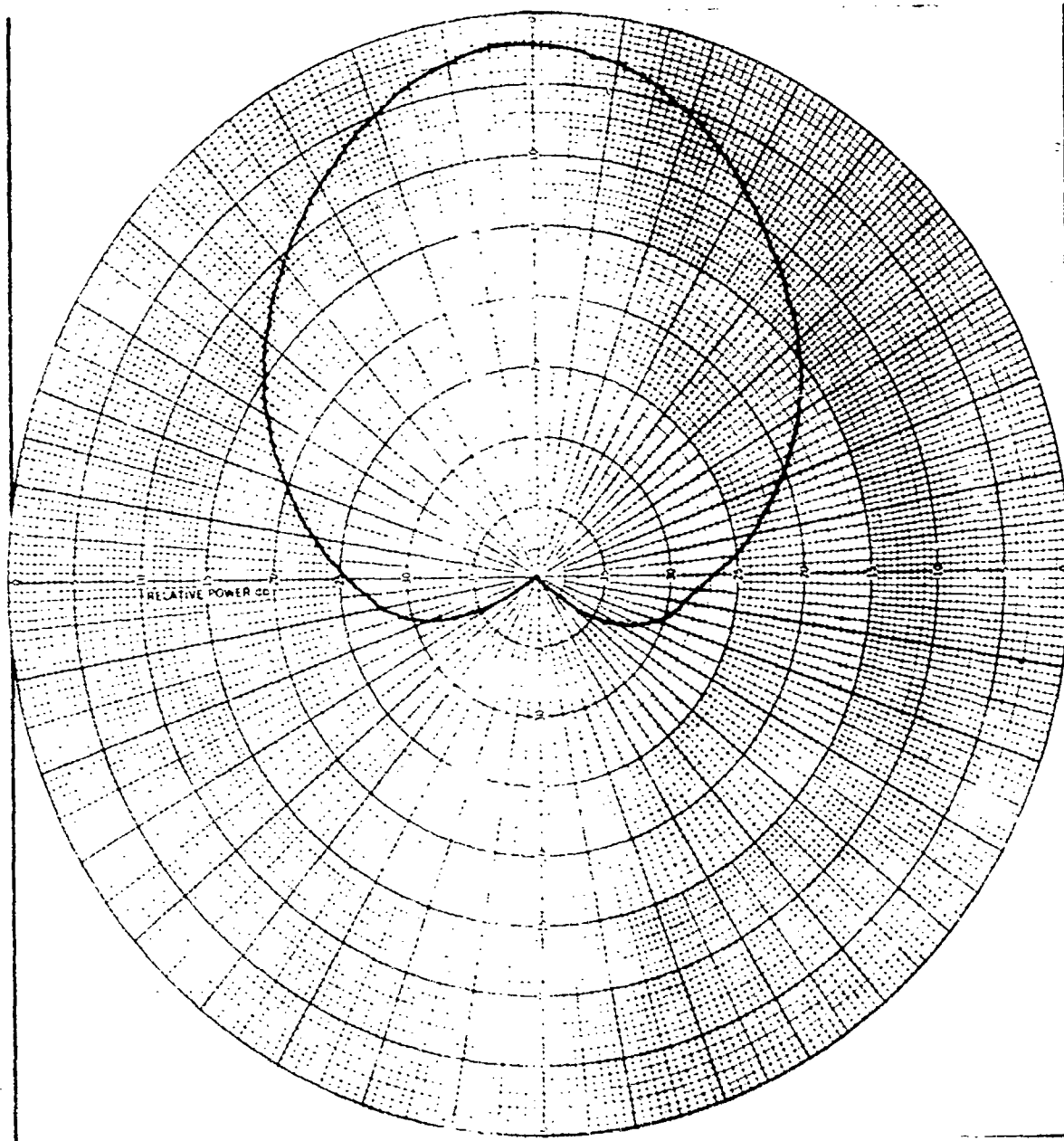


FIG. 15 Measured radiation pattern, L-band corner reflector antenna
1250 MHz, Elevation (H) plane

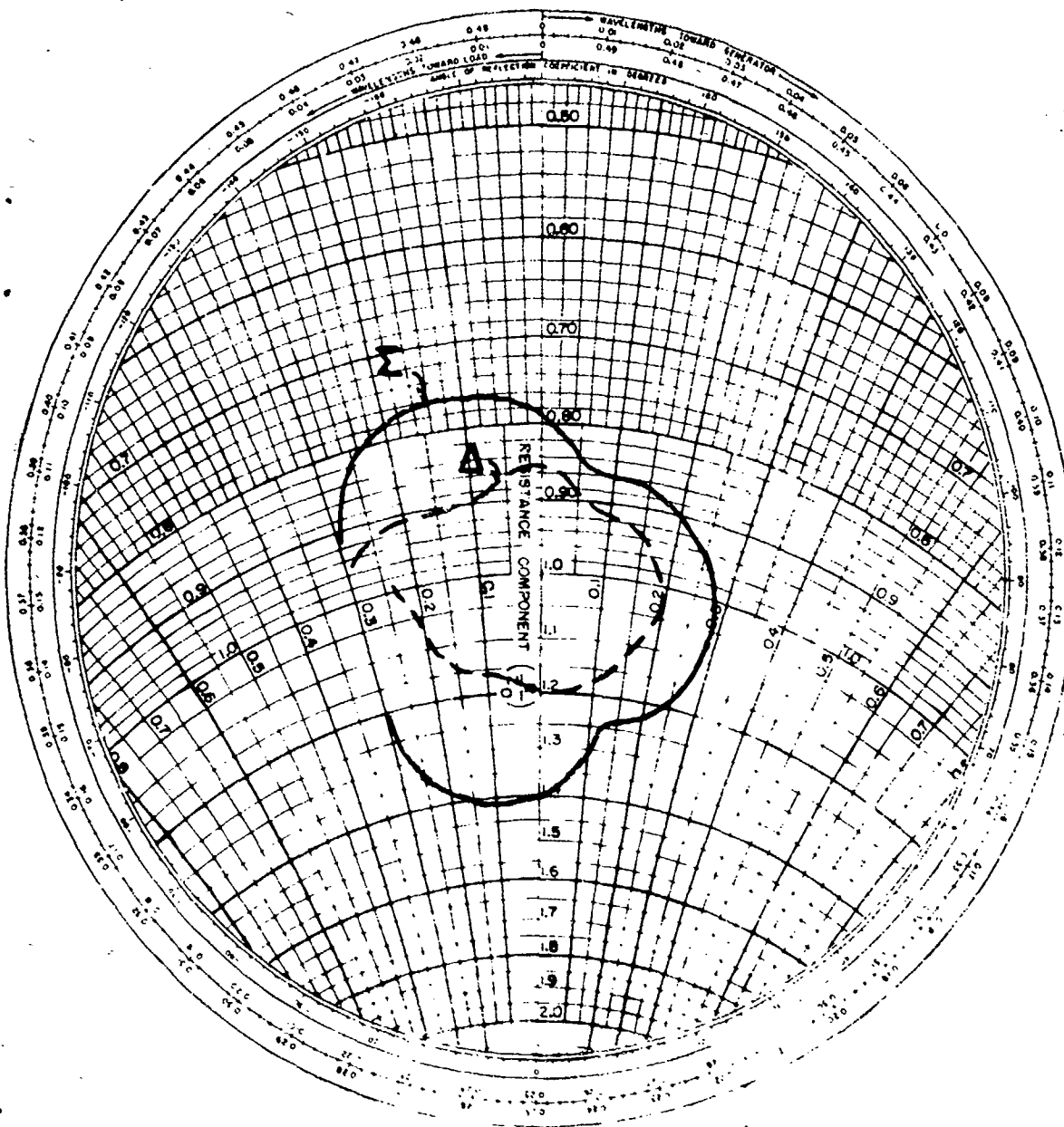


Fig. 16 Measured impedance, L-band corner reflector antenna
1200-1300 MHz

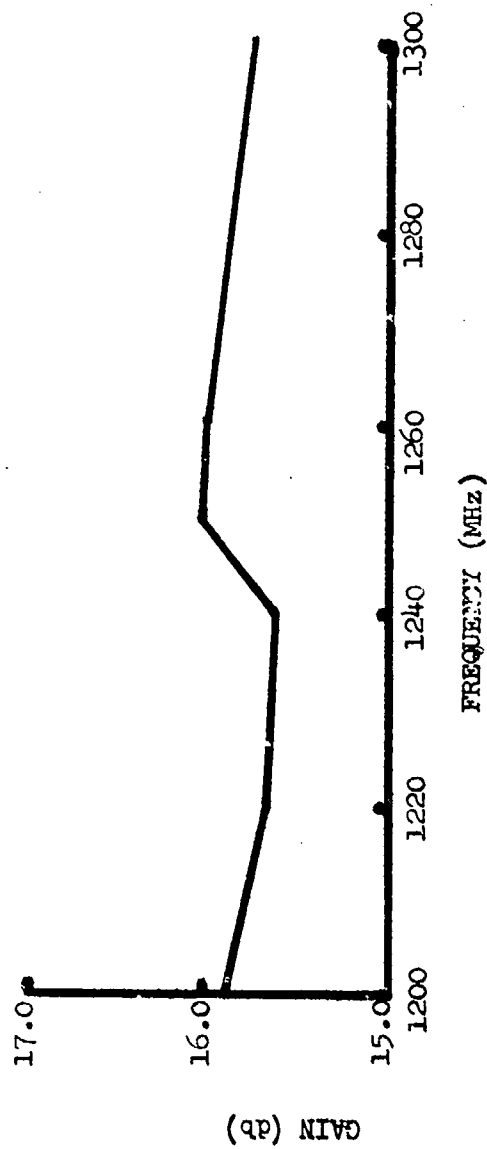


Fig. 17 L-band corner reflector antenna gain